Supplementary Information

The dynamic effect on mechanical contacts between nanoparticles

Weifu Sun*

1. Characterization of Silicon Nanospheres.

The atomic structures of silicon nanospheres are characterization as done before[1]. The results show that surface roughness rms, surface thickness δ and maximum surface thickness δ_{Max} can be regarded as independent of nanosphere radius. The defined particle radii $\overline{R}$ corresponding to R_0=1.0, 2.0, 3.0, 4.0 and 5.0 nm are 0.862, 1.876, 2.864, 3.839 and 4.849 nm, respectively. rms is about 0.63±0.02 Å, δ is about 1.65±0.08 Å, δ_{Max} is about 2.30±0.36 Å and $2\Delta d=2(R_0-R)$ is about 2.84±0.28 Å. For silicon nanospheres, there is almost no surface atoms fluctuating out of the cut-obtained radius R_0 since it always satisfies $R^{\mathrm{core}}+\delta_{\mathrm{Max}} \le R_0$. Therefore, for the sake of convenient discussion, it appears that the cut-obtained particle size R_0 is more appropriate than the defined particle size $\overline{R}$. Moreover, the influence of temperature on particle's structural parameters was also explored using the NVT ensemble for comparison. The results (Table S2) indicate that the change of temperature from 1 to 600 K only leads to a slight change of particle size (R) and surface roughness (rms). Therefore, the influence of temperature on the structure of a silicon nanosphere may be ignored and the defined structural parameters are considered to be independent of temperature.

Table S1. Structural parameters of silicon nanospheres at 300 K

R_0 (Å)	R^{core}(Å)	$\overline{R}$ (Å)	rms (Å)	rms/R	δ_{Max} (Å)	δ (Å)
10	7.75	8.62	0.65	0.075	1.78	1.52
20	17.7	18.76	0.61	0.033	2.14	1.68
30	27.55	28.64	0.62	0.022	2.39	1.66
40	37.25	38.39	0.65	0.017	2.75	1.74
50	47.45	48.49	0.61	0.013	2.45	1.65

Table S2. Structural parameters of silicon nanospheres of R_0= 2.0 nm at different temperature T.

T (K)	1	150	300	450	600
R^{core} (Å)	17.7	17.7	17.7	17.65	17.60
$\overline{R}$ (Å)	18.77	18.78	18.76	18.74	18.70
rms (Å)	0.60	0.60	0.61	0.63	0.64
rms/*R*	0.032	0.032	0.033	0.034	0.034
δ (Å)	1.67	1.68	1.68	1.72	1.74
δ_{Max} (Å)	2.02	2.18	2.14	2.28	2.34

Note: R_0 represents arbitrarily cut particle radius.

2. Effect of temperature on the LJ potential and mechanical contact forces

Figure S1-a shows that the results obtained at different temperatures ranging from 100 to 300 K are almost identical and the effect of temperature on the interparticle potentials can be ignored. Likewise, the results in Figure S1-b show that the mechanical contact forces obtained at different temperatures ranging from 100 to 300 K are almost identical, indicating that contact forces can be considered to be independent of temperature.

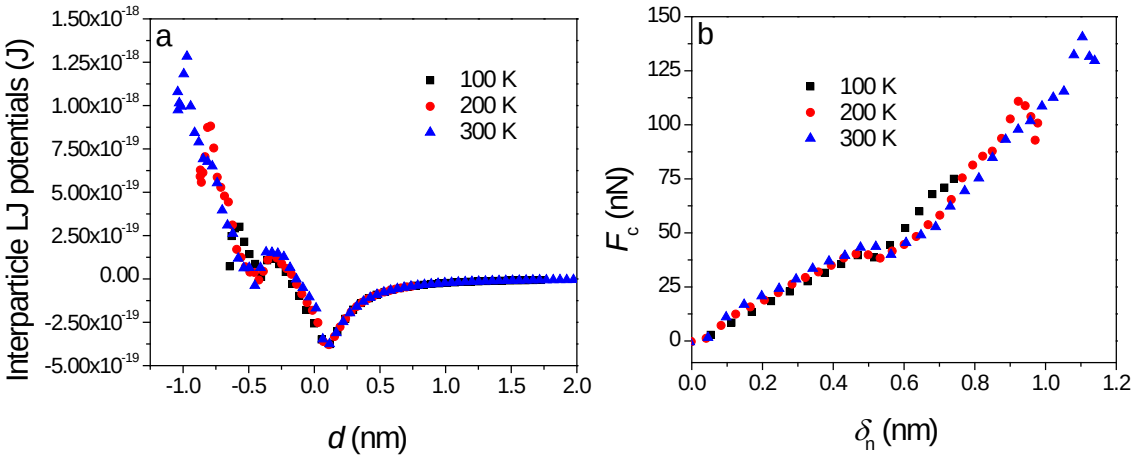

Figure S1. (a) Interparticle LJ potentials as a function of surface separation d and (b) mechanical contact forces as a function of normal displacement δ_n between silicon nanospheres of 2.0 in radius at an initial relative velocity of 100 m/s under different temperatures using NVT ensemble.

3. Measurement of Young's modulus of silicon bulk

The Young's modulus of silicon bulk was separately measured by MD simulations. MD simulations were performed on a simulation cell of $L \times M \times M$ nm^3 (L=8.0, M=6.0), which was filled with silicon molecules as bulk (Figure S2-a). After geometry optimization, MD simulation was first conducted using a NVT ensemble (i.e., constant number of atoms, constant volume and constant temperature) at 300.0 K running for at least 50.0 ps after equilibration. The equilibrated structure in the final frame was exported and then MD simulations were carried out using NPT ensemble (i.e., constant number of atoms, constant pressure and constant temperature) at 298.0 K for at least 50.0 ps along the (100) direction, following geometry optimization. A series of external pressures were applied along X-axis only, *i.e.*, the (100) direction, in order to obtain compressive stress-strain curve (Figure S2-b).

Young's modulus is derived from the initial linear part of the typical stress-strain curve (Figure S2-b) of silicon bulk. With increase in stress, the corresponding strain first increases linearly and then increases sharply. The slope of initial linear part (satisfying Hooke's law) was used to derive elastic modulus of ca. 125.5 GPa along the (100) direction of crystalline silicon bulk, which is 3.5% lower than experimental result of 130 GPa,[2] indicating an excellent agreement with each other.

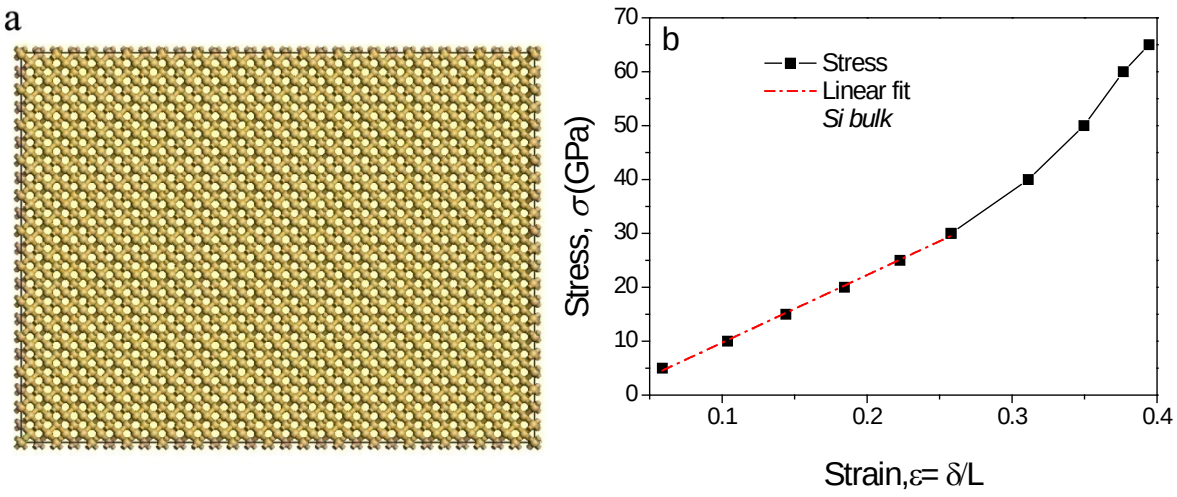

Figure S2. (a): Simulation model used to measure Young's modulus of silicon counterpart bulk along the (100) direction; (b): Compressive stress-strain curve of silicon bulk.

4. Contact Forces at low Impact Velocity.

The mechanical contact forces obtained at low impact velocities between silicon nanospheres of radii ranging from 1.0 to 5.0 nm are shown in Figure S3. The MD simulated results are in accordance with that predicted by the Hertz model using Young's modulus of silicon bulk.

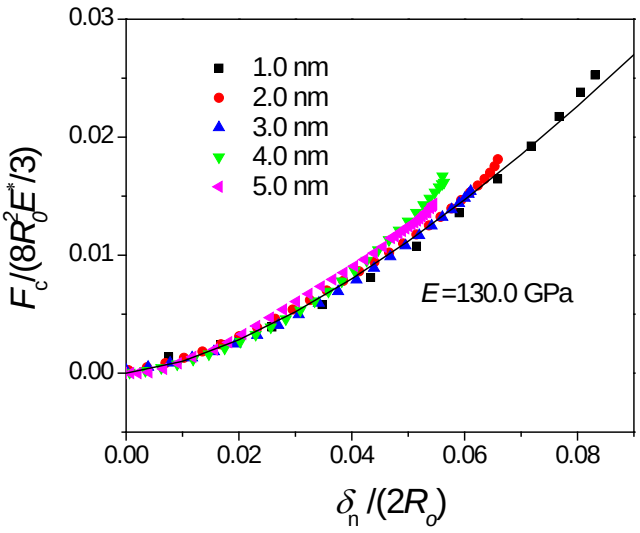

Figure S3. Normalized $F_c/(8R_0^2E^*/3)$ as a function of $\varepsilon=\delta_n/(2R_0)$ obtained in the approach process from the MD simulation between two silicon nanospheres of radii ranging from 1.0 to 5.0 nm at an initial relative velocity of $V_{r,0}$ = 2.0 Å/ps (i.e., 200 m/s). The zero value of δ_n corresponds to the first non-zero value of contact force. Solid line represents the Hertz prediction using Young's modulus of silicon bulk.

5. Origins of the Hardening Effect and Comparisons with Three Established Theories

First, the constraint-counting theory of the elastic properties of random covalent networks predicts that the Young's modulus should depend on mean atomic coordination Z, given by[3]

$$E = E_0\left(Z - 2.4\right)^{1.5} \qquad \text{(S-1)}$$

where E_0 =130 GPa. Z is the mean coordination. According to the data in Figure 2b, given the coordination radius is 3.0 Å, the number of atoms corresponding to CN=1, 2, 3, 4, 5, and 6 are 24, 150, 244, 1281, 8 and 2, respectively, thus the mean coordination coordination number is

Z=3.6465. Using Eq. (S-1), the apparent elastic modulus is about 180.9 GPa, which is still much smaller than 497.6 GPa.

Second, according to the bond-order-length-strength (BOLS) correlation mechanism,[4] the change in elastic modulus can be given by

$$\frac{\Delta E}{E_0} = \frac{E - E_0}{E_0} = c_i^{-(m+3)} - 1 \qquad \text{(S-2)}$$

where m=4.88 for silicon,[4] c_i is the change of bond length between before and after compression. Now take silicon nanospheres of 2.0 nm in radius for example, the bond length becomes shorten to around 2.20 Å while the original length is about 2.3516 Å, thus c_i=2.2/2.3516≈0.9355, using Eq. (S-2), the apparent elastic modulus is about E=219.84 GPa, which is still much smaller than the results obtained from MD simulations of 497.6 GPa.

Thirdly, according to one of the typical equations of state-Murnaghan relationship, the pressure effect on elastic modulus E can be related to compressive Young's modulus E_0 by

$$E = E_0 + \beta P_0 \qquad \text{(S-3)}$$

where β=3α(1-2ν), P_0 is the mean contact pressure, ν is Poisson ratio, E_0=130 GPa, ν= 0.28,[2] a value of α=4 is found to be valid for many materials and silicon in particular.[5] Now taking silicon nanospheres of 2.0 nm in radius for example, the mean contact pressure P_0 at $V_{r,0}$=1000 m/s is about 13.19 GPa (Table 2), therefore, the apparent elastic modulus E should be about 199.64 GPa, which is much smaller than 497.6 GPa (Table 1).

In short summary, any single of the three known theories cannot explain the higher elastic modulus obtained in present MD simulation. Probably, the three aspects together contribute to the hardening effect. This area awaits much more mature theory to consider the dynamic effect.

6. The Maximum Compression (or the Minimum Gap) Obtained at Normal Impact

The minimum gap (or the maximum compression) between silicon nanospheres during normal impact can be measured by MD simulations (Figure S4), given by

$$d_{\min}(\text{nm}) = 0.16 - 1.677 R_0 V_{r,\max}^{4/5} \left[\rho\left(1-\nu^2\right)/E_0\right]^{2/5} \qquad \text{(S-4)}$$

Since when two atoms or surfaces are less than equilibrium separation distance, which is about 0.165~0.2 nm, it can be considered in contact. Thus, assuming $\delta_n^* = -d_{min} + 0.16$, then Eq. (S-4) can be reduced to

$$\delta_n^* = 1.677 R_0 V_{r,max}^{4/5} \left[\rho \left(1-\nu^2\right) / E_0 \right]^{2/5} \qquad \text{(S-5)}$$

The Hertz continuum prediction of the maximum compression during normal impact between two frictionless elastic spheres is given by[6]

$$\delta_n^* = \left(\frac{15 m^* V^2}{16 \left(R_0^*\right)^{1/2} E^*} \right)^{2/5} \approx 1.985 R_0 V^{4/5} \left[\rho \left(1-\nu^2\right) / E_0 \right]^{2/5} \qquad \text{(S-6)}$$

The origins of the decrease of the coefficient in Eq. (S-6) can be attributed to the neglect of intermolecular repulsive forces and energy dissipations because of dynamic motions of atoms and plastic deformation of nanoparticles.

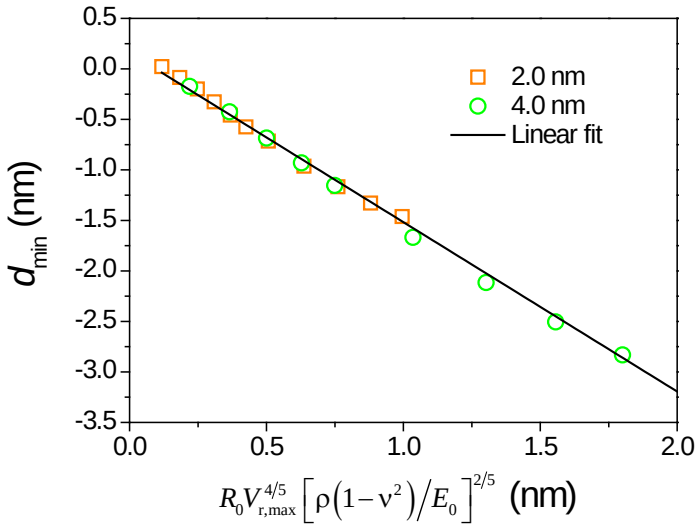

Figure S4. Dependence of the minimum gap between silicon nanosphere of radius 2.0 and 4.0 nm on the product of $R_0 V_{r,max}^{4/5} \left[\rho \left(1-\nu^2\right) / E_0 \right]^{2/5}$. Note that R_0, $V_{r,max}$, ρ, E_0 are in unit of nm, m/s, kg/m^3, Pa, respectively.

7. Origins of the Decrease of the Coefficient in Eq. (S-6).

The decrease of the coefficient from 1.985 to 1.677 is observed. In other words, given the same conditions, the amount of displacement predicted by Eq. (S-6) becomes smaller for nanoparticles than macroparticles. The origins of this difference are analyzed. Eq. (S-6) is obtained based on two frictionless elastic particles without considering intermolecular forces. But for nanoparticles, the following factors can contribute to the differences (Figure S5):

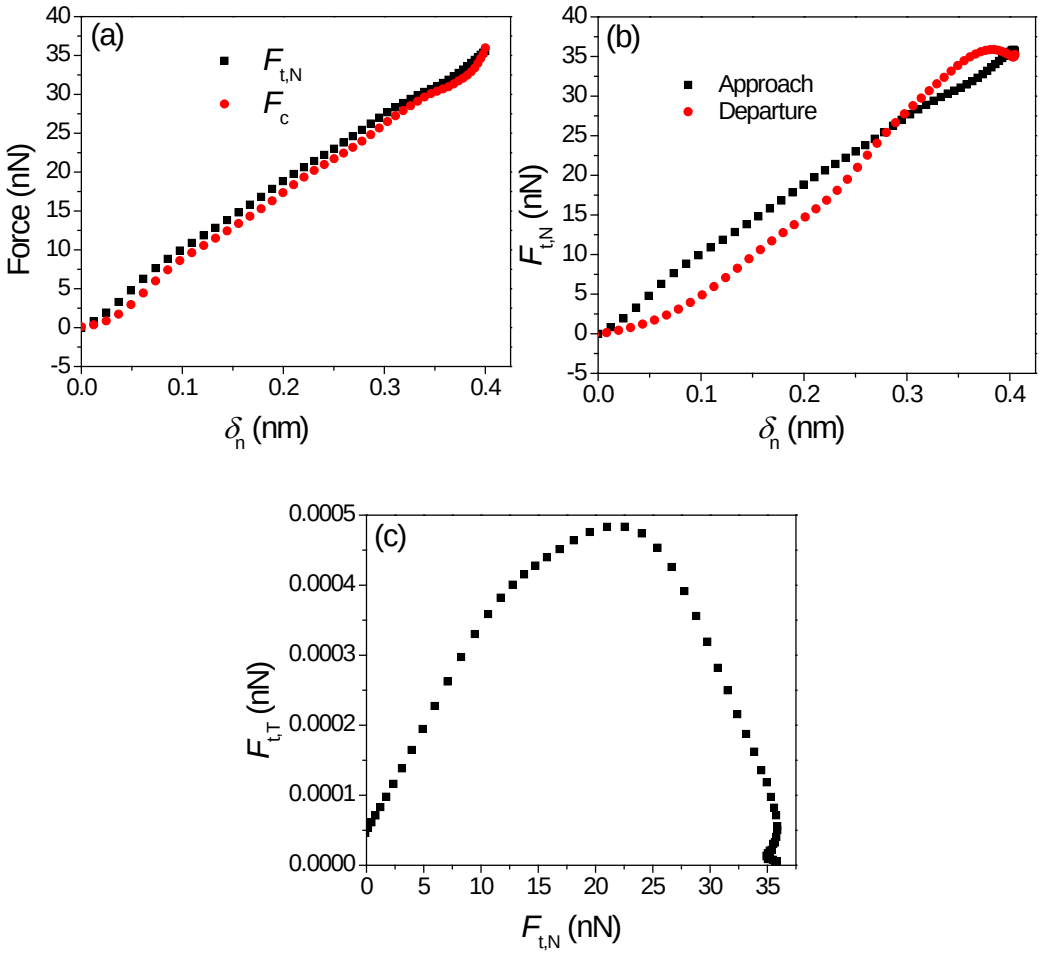

Figure S5. (a) total normal force $F_{t,\,N}$ and mechanical contact force F_c, also called 'elastic repulsive force'; (b) hysteresis phenomena in the $F_{t,\,N}$ obtained in the approach and departure process; (c) total tangential force $F_{t,\,T}$ versus $F_{t,\,N}$ between silicon nanospheres of 2.0 nm in radius. $V_{r,0}$=600 m/s.

First, the role of intermolecular forces after contact deformation is mainly repulsive. In other words, apart from the mechanical contact force which is repulsive in nature, there is an additional repulsive force exerting on nanoparticles compared to macroparticles. This can be

especially reflected from Figure S5-(a): the total normal force $F_{t,N}$ becomes more repulsive than mechanical contact force F_c.

Second, plastic deformation may happen after compression. This can be reflected from the hysteresis as shown in the inset of Figure S5-(b). It can be observed that serious hysteresis phenomenon occurs, indicating that the particle is plastically deformed in part and some energy has been dissipated into plastic deformation, reserved as strain energy. Note that the abnormal increase of normal force in the departing process between 0.3 and 0.4 nm may arise from the displacement and/or dislocation of contacting atoms of two opposing surfaces.

Last but not least, the energy dissipation due to the displacement of contacting atoms on the opposing surfaces, such as the thermal vibrations and/or dislocations of interacting atoms can lead to additional energy loss and hence the decrease of the coefficient. This can be reflected from the total tangential force as shown in Figure S5-(c). The total tangential force $F_{t,T}$ is given by

$$F_{t,T} = \sqrt{F_Y^2 + F_Z^2} \qquad \text{(S-7)}$$

where F_Y and F_Z are the accumulated forces along the Y and Z directions. (The two particles impact each other along X-axis, *i.e.*, the normal direction.)

References and notes

1 W. F. Sun, Q. H. Zeng and A. B. Yu, *Langmuir*, 2013, **29**, 2175-2184.

2 M. A. Hopcroft, W. D. Nix and T. W. Kenny, *J. Microelectromech. Syst.*, 2010, **19**, 229-238.

3 H. He and M. F. Thorpe, *Phys. Rev. Lett.*, 1985, **54**, 2107-2110.

4 C. Q. Sun, *Prog. Solid State Chem.*, 2007, **35**, 1-159.

5 W. M. Mook, J. D. Nowak, C. R. Perrey, C. B. Carter, R. Mukherjee, S. L. Girshick, P. H. McMurry and W. W. Gerberich, *Phys. Rev. B*, 2007, **75**, 214112-1-10.

6 K. L. Johnson, *Dynamic effects and impact*, Cambridge University Press, Cambridge, 1985.